De Novo Design of Selective Antibiotic Peptides by Incorporation of Unnatural Amino Acids

Rickey P. Hicks,* Jayendra B. Bhonsle, Divakaramenon Venugopal, Brandon W. Koser, and Alan J. Magill

Division of Experimental Therapeutics, Walter Reed Army Institute of Research 503 Robert Grant Avenue, Silver Spring, Maryland 20910

Received December 29, 2006

The evolution of drug-resistant bacteria is one of the most critical problems facing modern medicine and requires the development of new drugs that exhibit their antibacterial activity via novel mechanisms of action. One potential source of new drugs could be the naturally occurring peptides that exhibit antimicrobial activity via membrane disruption. To develop antimicrobial peptides exhibiting increased potency and selectivity against Gram positive, Gram negative, and Mycobacterium bacteria coupled with reduced hemolytic activity, peptides containing unnatural amino acids have been designed, synthesized, and evaluated. These compounds were designed on the basis of the electrostatic surface potential maps derived from the NMR determined SDS and DPC micelle-bound conformations of (Ala^{8,13,18})magainin-2 amide. Unnatural amino acids were incorporated into the polypeptide backbone to control the structural and physicochemical properties of the peptides to introduce organism selectivity and potency. The methods and results of this investigation are described below.

Introduction

Antimicrobial peptides (AMP[a]) have evolved in almost every class of living organism as a defense mechanism against invading microorganisms.[1,2] As of 2004,[3] over 800 antimicrobial peptides had been isolated and characterized from various organisms including humans,[4] amphibians,[5] insects, mammals, birds, fish, and plants.[2] AMPs are generally small (10−50 amino acid residues) and highly positively charged (+3 to +9)[6] amphipathic molecules with well-defined hydrophobic and hydrophilic regions.[3,7] The exact mechanism of lipid-induced cytotoxicity of these peptides is currently debated in the literature[8] with AMPs divided into two mechanistic classes, membrane disruptors and nonmembrane disruptors.[8,9] However, there is a general agreement that the first target for either membrane disruptor or nonmembrane disruptor AMPs is the negatively charged membranes of bacterial cells.[8] There are several different structural classes of membrane-disruptor AMPs, but for the purpose of this investigation we focused on linear amphipathic helical peptides. These peptides make up the most abundant class of AMPs with over 290 different peptides reported,[9,10] most exhibiting minimum inhibitory concentrations (MIC) for antibacterial activity in the low-micromolar range.[2,8] In many cases these peptides exhibit characteristics of a random coil conformation in aqueous or in organic solvents; however, on binding to micelles or membranes, they adopt an ordered amphipathic secondary structure.[11]

The α-helical structural class of membrane disruptors can be divided into two subclassifications based on biological activity: (1) cell selective and (2) nonselective.[12] As the name implies, cell selective AMPs exhibit potent activity against bacterial cells while being inactive against mammalian cells, and nonselective AMPs exhibit activity against bacterial as well as mammalian cells. A large number of investigations have focused on the development of cell selective AMPs[12−15] with varying degrees of success. In general, hemolytic activity correlates with high hydrophobicity, amphipathicity, and helicity.[15,3,16] Selective incorporation of D-amino acids, proline, peptoids, and amino acids with differing hydrophobicity can reduce the resulting hemolytic activity.[12,13,15,17]

To provide insight into the process of AMP cell type selectivity, one needs to look into their mechanism of action. All membrane disruptors follow specific steps during the process of interacting with and binding to the target cell's membranes.[18] The first step is the attraction (movement of the AMP though bulk solution to areas near the surface) of the AMP to the surface of the membrane.[9] The driving force for this attraction is the electrostatic interaction between the positively charged basic amino acids of the AMP and the negatively charged acidic phospholipids of the cell membrane.[2,11,19,20] The second step is binding of the AMP to the surface of the membrane.[9] In this step the AMP attaches to the surface of the membrane by locating the positively charged side chains relatively close to the negatively charged polar head groups of the phospholipids followed by insertion of the hydrophobic side chains of the AMP into the hydrophobic core of the membrane. During this process conformational changes occur on the AMP that stabilizes the attractive electrostatic and hydrophobic interactions concurrently minimizing the repulsive interactions between the AMP and the membrane.[3] At lower concentrations the long axis of the AMP is oriented parallel to the surface of the membrane called the S-state[21] (surface). As the concentration of the AMPs increases on the surface of the membrane, a critical concentration is reached where the peptides self-assemble to form complexes of four to six AMPs. This induces a change in the orientation of the long axis of the AMPs from parallel to perpendicular relative to the surface of the membrane, resulting in the insertion of the assembled AMPs into the membrane and forming a transmembrane pore called the I-state (inserted).[9,22]

On the basis of the above theory, the observed selectivity of AMPs for prokaryotic vs eukaryotic cells must be derived from one of two possible scenarios. (1) The AMP is not attracted by electrostatic interactions to the surface of the membrane, and therefore, the S-state is not formed. (2) If the S-state is formed, then self-assembly of the AMPs to the I-state does not occur,

* To whom correspondence should be addressed. Current address: Department of Chemistry, East Carolina University, Science and Technology Building, Suite 300, Greenville, North Carolina 27858. Telephone: 252-328-9700. Fax: 252-328-6210. E-mail:hicksr@ecu.edu.

[a] Abbreviations: Ahx, 6-aminohexanoic acid; AMP, antimicrobial peptide; βAla, β-alanine; Dpr, diaminopropionic acid; Fpa, 4-fluorophenylalanine; GABA, γ-aminobutyric acid; Nph, 4-nitrophenylalanine; Oic, octahydroindolecarboxylic acid; Tic, tetrahydroisoquinolinecarboxylic acid.

10.1021/jm061489v
Published on Web 06/05/2007

preventing transmembrane pore formation. In either case it is the interaction between the physicochemical properties of the AMP and the membrane that determines whether the S-state and I-state are formed. This observation is consistent with current discussion in the literature that speculates that the selectivity for bacterial vs mammalian cells is believed to be based on the differences in the chemical composition of the two cell membranes.[2,3] Bacterial cells contain a high percentage of negatively charged phospholipids, while mammalian cells contain a much higher concentration of zwitterionic phospholipids.[23] Other differences also exist, including membrane composition (sterols, lipopolysaccharide, peptidoglycan, etc.),[1] structure, transmembrane potential, and polarizability. These differences are in part responsible for the observed selectivity of some AMPs for bacterial vs mammalian cells.[6,24] In addition to the differences between eukaryotic and prokaryotic cells, the membranes surrounding different types of bacteria are also different. The lipid bilayer of Gram positive bacteria is covered by a porous layer of peptidoglycan, while the structure of Gram negative bacteria is more complex with two lipid membranes containing lipopolysaccharides and porins.[2,25] The outer membrane of mycobacteria is the most complex consisting of a very thick mycolate-rich outer coat[26] that is very difficult to penetrate. There is a developing preponderance of evidence in the literature supporting the concept that the selectivity and potency of a specific AMP are determined in a large measure by the chemical composition of the target membrane.[8,24] Thus, it is reasonable to postulate that the membrane's physicochemical surface interactions with the physicochemical surface of the AMP define organism selectivity.[2,8,25,27] The hypothesis guiding our research was developed from this observation. The physicochemical properties of the target cell's membrane interact with the physicochemical properties of the approaching AMP defining its selectivity and potency against that particular cell. During this process conformational changes are induced onto the AMP that will maximize the attractive interactions between the two to facilitate AMP-membrane binding.

Analogues of the magainin family of host defense peptides were selected to evaluate this hypothesis because these peptides are active against Gram positive and negative bacteria, fungi, and protozoa while exhibiting little mammalian cell toxicity.[28] The interactions of the magainins[29−31] with membrane models have been extensively investigated, resulting in the characterization of the magainins as well-defined α-helical amphipathic cell-selective membrane disruptors. A great deal of what is known about the mechanisms of antibacterial activity is based on investigations of AMP interactions with model membrane systems.[9] These interactions can be characterized using various types of spectroscopy including NMR,[32−34] circular dichroism,[35] Fourier transform infrared spectroscopy,[36] and Raman spectroscopy.[37] Because of our previous experience,[38−41] we selected NMR as the method of choice for this investigation. For this preliminary investigation, DPC micelles[42] were selected as a simple model for zwitterionic lipids and SDS micelles[43] were selected as a simple model for anionic lipids. We previously reported two-dimensional NMR and molecular modeling[11] investigations conducted in our laboratory that indicated that (Ala[8,13,18])magainin-2 amide bound to DPC micelles adopts an α-helical structure involving residues 2−16 with the four C-terminal residues converging to a loose β-turnlike structure, while (Ala[8,13,18])magainin-2 amide bound to SDS micelles adopts an α-helical structure involving residues 7−18 with the C- and N-terminal residues exhibiting a great deal of conformational flexibility. The most plausible cause for this observation is that different noncovalent (electrostatic and hydrophobic) interactions are occurring between the peptide's surface and the two micelle surfaces. The results of our previous research into peptide−micelle interactions provided the following insight: (1) Electrostatic interactions are responsible for peptide−micelle binding, while hydrophobic interactions are responsible for inducing a stable secondary structure onto the peptide.[44,45] (2) The electrostatic interaction that occurs between cationic peptides and zwitterionic micelles, such as DPC, are more "complex" than those that occur with anionic micelles, such as SDS.[45] The reason for this behavior is that the counterions for anionic micelles in this case (SDS) are Na^+ ions, which are not covalently linked to the SDS. Hence, they are free-flowing in solution and in turn are easily displaced by the positively charged side chains of the incoming peptide. However, for the zwitterionic micelle the counterions are covalently bound to each other. Thus, the positive and negative charges of the zwitterionic micelle have limited freedom of motion. As the positive charges of the incoming peptide approaches the surface of the zwitterionic micelle, the positive counterions of the micelle cannot be displaced from the surface and are forced to diffuse into solution away from the micelle, as was the case with anionic micelles. Therefore, both attractive electrostatic interactions between the positive charges on the peptide and the negative charges on the micelle as well as the repulsive electrostatic interactions between the positive charges on the peptide and the positive charges on the micelle will be inversely synergistic in nature and are not mutually exclusive.[45] Thus, the binding process will require the conformation of the incoming peptide to adapt in response to these interactions in order to maximize the attractive interactions concurrently minimizing the repulsive interactions. We and others have observed that the position in three-dimensional space of each of the multiple positive charges on the peptide relative to the hydrophobic residues controls the allowable conformational changes.[45] Therefore, electrostatic interactions between the polar head groups of the micelle and the cationic side chains of the peptides define the positions along the peptide backbone where the helical structures begin and end.

By use of the NMR-determined SDS and DPC micelle bound conformations of (Ala[8,13,18])magainin-2 amide, the electrostatic surface potential maps calculation for these conformers indicated that the surface electron density of these peptides is highly conformation-dependent.

Results

The different physicochemical surface properties of the SDS and DPC micelle-bound conformations of (Ala[8,13,18])magainin-2 amide were used to design a novel class of AMPs. These AMPs contain both natural and unnatural amino acids that induce a semirigid conformation onto the peptide backbone, thus controlling the three-dimensional physiochemical properties of the peptide. In our laboratory we are using the two unnatural amino acids Tic and Oic to induce an amphipathic and a loose α-helical structure. Kyle and co-workers reported, using NMR and molecular modeling methods, that the dipeptide Tic−Oic, when placed in positions $i + 1$ and $i + 2$ of a four amino acid sequence, induced a β-turn.[46] We hypothesized that placement of multiple Tic−Oic units connected via two amino acid spacers with defined properties of charge and hydrophobicity will result in peptides with well-defined physiochemical properties while maintaining sufficient conformational flexibility to allow interactions with membranes of different physicochemical properties.

The basic polypeptide skeleton of the new AMPs is given in Figure 1. This skeleton begins with a turn-inducing Tic−Oic

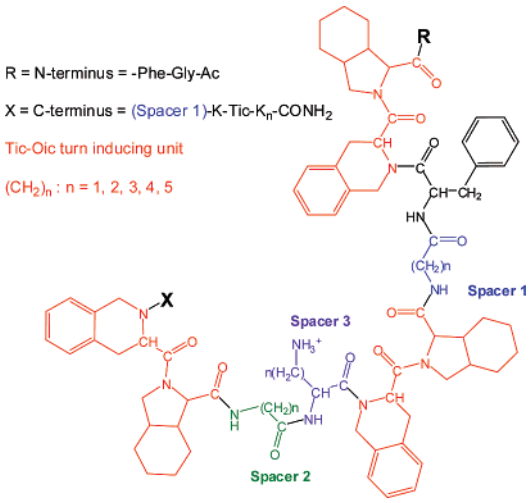

Figure 1. Diagrammatic representation of the basic skeleton units of AMPs developed in our laboratory.

unit coupled to a spacer amino acid followed by an amino acid with a cationic side chain. This is followed by another Tic−Oic unit coupled to a spacer followed by a hydrophobic amino acid residue. Preliminary 1D ^{1}H NMR investigations confirmed that these AMPs have sufficient structural flexibility to undergo significant conformational changes on interacting with membranes with different physicochemical properties, such as SDS and DPC micelles. The effect of binding to DPC and SDS micelles is illustrated in Figure 2. The 600 MHz ^{1}H NMR spectrum shows the amide and aromatic region of two peptides bound to SDS and DPC micelles. Spectrum A is the antibacterial peptide **23** bound to DPC micelles, and spectrum B is the same peptide bound to SDS micelles. Clearly these two spectra are very different, and the most likely explanation for this observation is that the peptides exist in two different conformations. The broadening in the resonances of compound **23** bound to SDS micelles, particularly the aromatic resonances, indicates restricted motion of the phenyl rings, which is consistent with a "tighter" binding to the micelle. Also shown in Figure 2 are the spectra of the inactive analogue **8** bound to DPC (spectrum C) and SDS (spectrum D) micelles. Again, these spectra are different, indicating that the peptide exists in two different conformations. However, the line widths of both spectra are narrower than those observed for compound **23**, indicating that even though compound **8** binds to both micelles, it has a greater degree of molecular flexibility. A more rigorous structural NMR investigation is ongoing in our laboratory.

To date, 49 new AMPs have been synthesized, and Table 1 shows their amino acid sequences. To evaluate the antibacterial activity of these compounds, the following four bacterial strains were selected. (1) *Salmonella typhimurium* (ATCC 13311) because of its clinical relevance to the evaluation of activity against Gram-negative bacteria; (2) *Staphylococcus aureus* ME/GM/MTC resistant bacteria (ATCC 33592) because of its clinical relevance to the evaluation of activity against drug-resistant Gram positive bacteria; (3) *Mycobacterium ranae* (ATCC 110) because it is a commercially available screen for mycobacterium that hopefully will provide insight into activity against tuberculosis; (4) *Bacillus subtillis* (ATCC 43223) because it is a commercially available screen that will hopefully provide insight into activity against *Bacillus anthraces*.

The results obtained from these assays are given in Table 2, and these compounds exhibit a broad spectrum of antibacterial and hemolytic activity. The observed minimum inhibitory concentrations (MIC) for many of these analogues are as low as, or lower than, those reported for other AMPs against *Staphylococcus aureus* strains,[47−49] Gram-negative strains,[50] and mycobacterium strains.[48] Many of these compounds are very

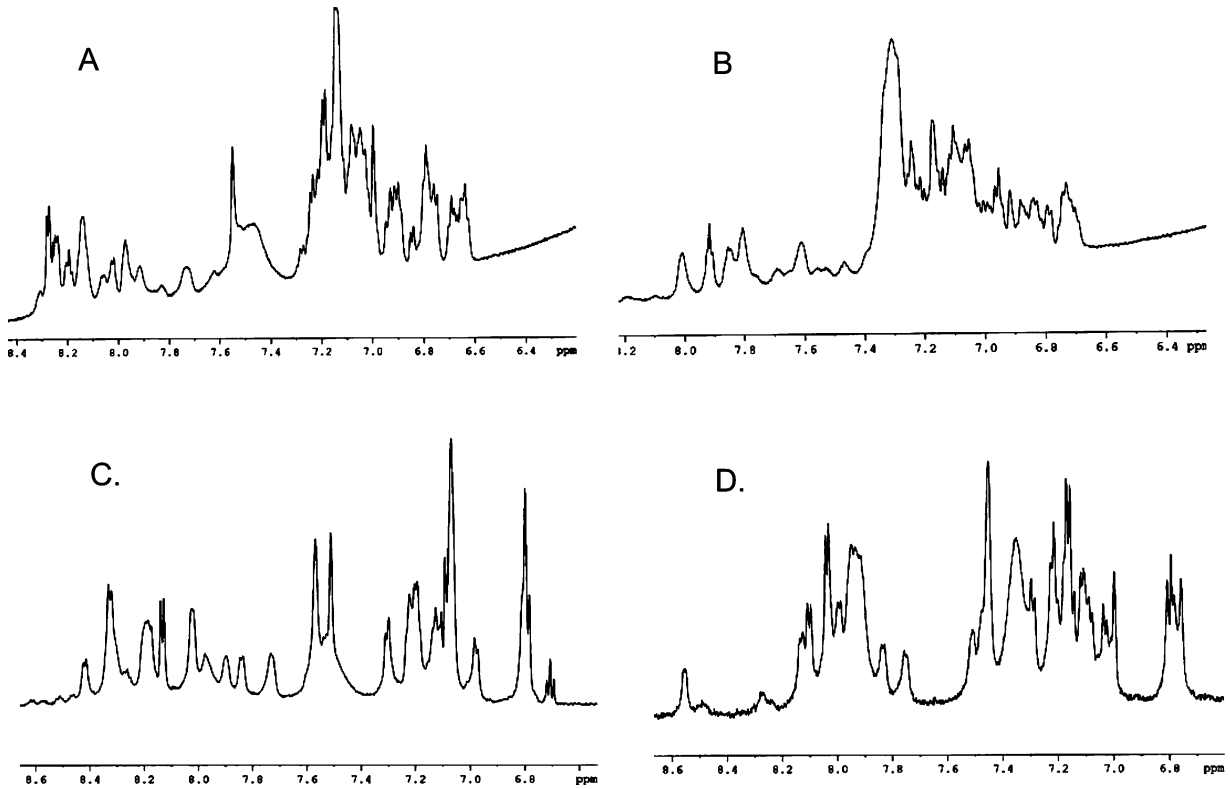

Figure 2. Amide and aromatic regions of the 600 MHz ^{1}H NMR spectra of two peptides bound to SDS and DPC micelles. Spectrum A is the antibacterial peptide **23** bound to DPC micelles, and spectrum B is the same peptide bound to SDS micelles. Spectrum C is the inactive peptide **8** bound to DPC micelles, and spectrum D is the same peptide bound to SDS micelles.

Table 1. Amino Acid Sequences for the Novel Antimicrobial Peptides Synthesized

peptide	amino acid sequence[a]
1	H_2N-GKGL-Tic-Oic-GK-Tic-Oic-GF-Tic-Oic-GK-Tic-Oic-GF-Tic-Oic-GK-Tic-Oic-GKR-$CONH_2$
2	H_2N-GKGL-Tic-Oic-GR-Tic-Oic-GF-Tic-Oic-GR-Tic-Oic-GF-Tic-Oic-GR-Tic-Oic-GKR-$CONH_2$
3	H_2N-GKGL-Tic-Oic-GL-Tic-Oic-GK-Tic-Oic-GL-Tic-Oic-GK-Tic-Oic-GL-Tic-Oic-GLR-$CONH_2$
4	H_2N-GKGL-Tic-Oic-GK-Tic-Oic-GL-Tic-Oic-GK-Tic-Oic-GL-Tic-Oic-GK-Tic-Oic-GKR-$CONH_2$
5	H_2N-GKGL-Tic-Oic-FK-Tic-Oic-KF-Tic-Oic-FK-Tic-Oic-KF-Tic-Oic-FK-Tic-Oic-FKR-$CONH_2$
6	H_2N-GKGL-Tic-Oic-GR-Tic-Oic-GF-Tic-Oic-GR-Tic-Oic-GF-Tic-Oic-ELMNS-$CONH_2$
7	H_2N-ELMNS-Tic-Oic-GL-Tic-Oic-GK-Tic-Oic-GL-Tic-Oic-GK-Tic-Oic-ELMNS-$CONH_2$
8	H_2N-ELMNS-Tic-Oic-GKLGK-Tic-Oic-ELM S-$CONH_2$
9	H_2N-ELS-Tic-Oic-GKG-Tic-Oic-LKES-$CONH_2$
10	H_2N-ELMNS-Tic-Oic-GL-Tic-Oic-GK-Tic-Oic-GL-Tic-Oic-GK-Tic-Oic-ELMNR-$CONH_2$
11	H_2N-GKM FPGLGKFPGLGKFPELMGR- $CONH_2$
12	H_2N-GKM-Tic-Oic-GLGK-Tic-Oic-GLGK-Tic-Oic-ELMGR-$CONH_2$
13	Ac-GKMFPGLGKEFGLGKFPELMGER-$CONH_2$
14	Ac-GK-Tic-Oic-GLGKE-Tic-Oic-GLGK-Tic-Oic-ELMGER-$CONH_2$
15	H_2N-GKM-Tic-PGLGK-Tic-PGLGK-Tic-PELMGR-$CONH_2$
16	H_2N-GKM-Tic-Oic-G-Ahx-GK-Tic-Oic-G-Ahx-GK-Tic-Oic-ELMGR-$CONH_2$
17	H_2N-GKM-Oic-PGLGK-Oic-PGLGK-Oic-PELMGR -$CONH_2$
18	H_2N-GKM-Oic-GLGK-Oic-GLGK-Oic-ELMGR-$CONH_2$
19	H_2N-GKM-Tic-GLGK-Tic-GLGK-Tic-ELMGR-$CONH_2$
20	H_2N-GKGL-Tic-Oic-βAla-K-Tic-Oic-βAla-F-Tic-Oic-βAla-K-Tic-Oic-βAla-F-Tic-Oic-ELMNS-$CONH_2$
21	H_2N-EGKGLG-βAla-βAla-K-Tic-Oic-βAla-F-Tic-Oic-βAla-E-Tic-Oic-βAla-F-Tic-Oic-ELMNS-$CONH_2$
22	H_2N-KL-Tic-Oic-K-Tic-Oic-F-Tic-Oic-K-Tic-Oic-F-Tic-Oic-K-Tic-Oic-KR-$CONH_2$
23	Ac-GF-Tic-Oic-GK-Tic-Oic-GF-Tic-Oic-GK-Tic-KKKK-$CONH_2$
24	Ac-GF-Tic-Oic-GK-Tic-Oic-GF-Tic-Oic-GK-Tic-KKKK-CONH-CH_2-CH_2-NH_2
25	Ac-GF-Tic-Oic-GK-Tic-Oic-GF-Tic-Oic-GK-Tic-KKKK-CONH-CH_2-CH_2-CH_2-NH_2
26	H_2N-GF-Tic-Oic-GK-Tic-Oic-GF-Tic-Oic-GK-Tic-KKKK-$CONH_2$
27	H_2N-KL-Tic-Oic-GK-Tic-Oic-GF-Tic-Oic-GK-Tic-KKKK-$CONH_2$
28	Ac-F-Tic-Oic-K-Tic-Oic-F-Tic-Oic-K-Tic-KKKK-$CONH_2$
29	Ac-GABA-F-Tic-Oic-GABA-K-Tic-Oic-GABA-F-Tic-Oic-GABA-K-Tic-KKKK-$CONH_2$
30	Ac-G-Tic-Oic-K-Tic-Oic-G-Tic-Oic-K-Tic-KKKK-$CONH_2$
31	Ac-GF-Oic-GK-Oic-GF-Oic-GKKKKK-$CONH_2$
32	Ac-GF-Tic-GK-Tic-GF-Tic-GK-Tic-KKKK-$CONH_2$
33	Ac-GF-Tic-G-GK-Tic-G-GF-Tic-G-GK-Tic-KKKK-$CONH_2$
34	Ac-GF-G-Oic-GK-G-Oic-GF-G-Oic-GK-G-KKKK-$CONH_2$
35	Ac-GF-F-Oic-GK-F-Oic-GF-F-Oic-GK-F-KKKK-$CONH_2$
36	Ac-βAla-F-Tic-Oic-βAla-K-Tic-Oic-βAla-F-Tic-Oic-βAla-K-Tic-KKKK-$CONH_2$
37	Ac-Ahx-F-Tic-Oic-Ahx-K-Tic-Oic-Ahx-F-Tic-Oic-Ahx-K-Tic-KKKK-$CONH_2$
38	Ac-F-Tic-Oic-K-Tic-Oic-F-Tic-Oic-K-Tic-KKKKKK-$CONH_2$
39	Ac-GF-Tic-Oic-GK-Tic-Oic-GF-Tic-Oic-GK-Tic-KKKKK-$CONH_2$
40	Ac-GABA-F-Tic-Oic-GABA-K-Tic-Oic-GABA-F-Tic-Oic-GABA-K-Tic-KKKKK-$CONH_2$
41	Ac-GF-Tic-Oic-GK-Tic-Oic-GF-Tic-Oic-GK-Tic-Orn—Orn-Orn—Orn-$CONH_2$
42	Ac-G-Fpa-Tic-Oic-GK-Tic-Oic-G-Fpa-Tic-Oic-GK-Tic-KKKK-$CONH_2$
43	Ac-GF-Tic-Oic-G-Orn-Tic-Oic-GF-Tic-Oic-G-Orn-Tic-Orn—Orn-Orn—Orn-$CONH_2$
44	Biotin-GF-Tic-Oic-GK-Tic-Oic-GF-Tic-Oic-GK-Tic-KKKK-$CONH_2$
45	Ac-GF-Tic-Oic-G-Dpr-Tic-Oic-GF-Tic-Oic-G-Dpr-Tic-Dpr-DprDpr-Dpr-$CONH_2$
46	Ac-βAla-Fpa-Tic-Oic-βAla-Dpr-Tic-Oic-βAla-Fpa-Tic-Oic-βAla-Dpr-Tic-Dpr-Dpr-Dpr-Dpr-$CONH_2$
47	Ac-G-f-Tic-Oic-GK-Tic-Oic-G-f-Tic-Oic-GK-Tic-KKKK-$CONH_2$
48	Ac-GF-Tic-Oic-G-k-Tic-Oic-GF-Tic-Oic-G-k-Tic-KKKK-$CONH_2$
49	Ac-G-Nph-Tic-Oic-GK-Tic-Oic-G-Nph-Tic-Oic-GK-Tic-KKKK-$CONH_2$

[a] Tic, tetrahydroisoquinolinecarboxylic acid, Oic, octahydroindolecarboxylic acid, βAla, β-alanine, Dpr, diaminopropionic acid, Fpa, 4-fluorophenylalanine, Nph, 4-nitrophenylalanine, GABA, γ-aminobutyric acid, Ahx, 6-aminohexanoic acid, k, D-lysine, f, D-phenylalanine, Ac, acetyl.

active (0.3−1 μM) against the Gram positive *Bacillus subtillis* strain, exhibiting very similar activity to the helical peptoid mimics of magainin-2 amide reported by Patch and Barron.[51] As a reference, magainin-1 was also screened against three of these bacterial strains at concentrations as high as 100 μM. In these assays magainin-1 exhibited activity against *Salmonella typhimurium* only. As a point of reference, literature MIC values for magainin analogues against *Staphylococcus aureus*[52,53] and *Bacillus subtillis*[54,55] are included in Table 2. These analogues of magainin exhibited activity similar to the activity of our compounds.

As stated previously, these compounds were engineered to mimic the electrostatic surface potential of (Ala[8,13,18])magainin-2 amide. In Figure 3 the electrostatic surface potential map for one of the most active analogues, compound **23** (activity against *Salmonella typhimurium* is 10 μM; activity against *Staphylococcus aureus* ME/GM/MTC resistant bacteria is 3 μM; activity against *Mycobacterium ranae* is 10 μM), is shown, which clearly indicates that the compound is highly charged and amphipathic. By contrast, the electrostatic surface potential map for the much less active analogue **31** (activity against *Salmonella typhimurium* is 100 μM; there is no activity against *Staphylococcus aureus* ME/GM/MTC resistant bacteria; activity against *Mycobacterium ranae* is 100 μM) shown in Figure 4 clearly indicates that the compound is highly charged but the charge is not localized onto any one face of the molecule, and therefore, the molecule is not amphipathic. It is interesting to note that incorporation of the negatively charged pentapeptide (ELMNS) found at the C-terminus of the magainins at either the C-terminus or the N-terminus, or both, of these analogues not only dramatically reduced the hemolytic activity but also eliminated the antibacterial activity. The effect of incorporation of this pentapeptide sequence at both the C and N terminuses is shown by the electrostatic potential map of the completely inactive analogue **7** in Figure 5. Figure 5 suggests that these inactive analogues are neither highly charged nor amphipathic.

In addition to exhibiting activity against a broad spectrum of bacteria in vitro, these compounds have also shown activity in

Table 2. Minimum Inhibitory Concentration for Antimicrobial and Hemolytic Activity (100 and 25 μM)

peptide	*Salmonella typhimurium*	*Staphylococcus aureus* ME/GM/TC resistant bacteria	*Mycobacterium ranae*	*Bacillus subtillis*	hemolysis 100/25 μM
1	not active	10 μM/35 μg/mL	not tested	not tested	
2	100 μM/360 μg/mL	10 mM/36 μg/mL	not active	1 μM/3.6 μg/mL	100%
3	not active	100 μM/340 μg/mL	not tested	not tested	100%
4	100μM/350 μg/mL	10 μM/35 μg/mL	not tested	not tested	100%
5	100 μM/400 μg/mL	30 μM/120 μg/mL	not active	3 μM/12 μg/mL	100%
6	not tested	not tested	not tested	not tested	70%
7	not active	not active	not tested	not tested	3%
8	not active	not active	not tested	not tested	23%
9	not tested	not tested	not tested	not tested	23%
10	not tested	not tested	not tested	not tested	not tested
11	not active	not active	not tested	not tested	not tested
12	not tested	not tested	not tested	not tested	not tested
13	not active	not active	not tested	not tested	not tested
14	not active	not active	not tested	not tested	not tested
15	not active	not active	not tested	not tested	not tested
16	not active	not active	not tested	not tested	not tested
17	not active	not active	not tested	not tested	not tested
18	not active	not active	not tested	not tested	not tested
19	not active	not active	not tested	not tested	not tested
20	not active	not active	not tested	not tested	55%
21	not tested	not tested	not tested	not tested	27%
22	not active	10 μM/31 μg/mL	30 μM/93 μg/mL	1 μM/3.1 μg/mL	63%
23	10 μM/24 μg/mL	3 μM /7.2 μg/mL	10 μM/24 μg/mL	1 μM/2.4 μg/mL	14%
24	10 μM/25 μg/mL	3 μM /7.5 μg/mL	10 μM/25 μg/mL	1 μM/2.5 μg/mL	not tested
25	30 μM/75 μg/mL	10 μM/25 μg/mL	10 μM/25 μg/mL	3 μM/7.5 μg/mL	not tested
26	3 μM/7.2 μg/mL	10 μM/24 μg/mL	10 μM/24 μg/mL	1 μM/2.4 μg/mL	33.4%/14.3%
27	3 μM /7.5 μg/mL	30 μM 75 μg/mL	3 μM/7.5 μg/mL	1 μM 2.5 μg/mL	43.6%/24.9%
28	10 μM/22 μg/mL	3 μM/6.6 μg/mL	30 μM/66 μg/mL	1 μM/2.2 μg/mL	86.8%/50%
29	100 μM/280 μg/mL	10 μM/28 mg/mL	10 μM/28 mg/mL	1 μM/2.8 μg/mL	10.8%/1.0%
30	10 μM/20 μg/mL	10 μM/20 μg/mL	3 μM/6.0 μg/mL	1 μM/2.0 μg/mL	26.7%/9.2%
31	100 μM/180 μg/mL	not active	100 μM/180 μg/mL	3 μM/5.4 μg/mL	5.9%/3.2%
32	100 μM/200 μg/mL	not active	30 μM/60 μg/mL	10 μM/20 μg/mL	6%/4.9%
33	100 μM/220 μg/mL	not active	30 μM/66 mg/ mL	10 μM/22 μg/mL	5.70%/3.80%
34	not active	not active	100 μM/200 μg/mL	30 μM/60 μg/mL	3.30%/3.3%
35	10 μM/24 μg/mL	10 μM/24 μg/mL	10 μM/24 μg/μL	3 μM/7.2 μg/mL	27.30%/8.9%
36	10 μM/25 μg/mL	10 μM/25 μg/mL	1 μM/2.5 μg/mL	1 μM/2.5 μg/mL	24.4%/7.4%
37	10 μM/27 μg/mL	10 μM/27 μg/mL	3 μM/8.1 μg/mL	1 μM/2.7 mg/mL	44.7%/26.6%
38	10 μM/25 μg/mL	3 μM/7.5 μg/mL	3 μM/7.5 μg/mL	1 μM/2.5 μg/mL	41.3%/33.5%
39	10 μM/26 μg/μL	3 μM/7.8 μg/mL	3 μM/7.8 μg/mL	1 μM/2.6 μg/mL	24.9%/18.9%
40	10 μM/27 μg/μL	30 μM/81 μg/mL	3 μM/8.1 μg/mL	1 μM/2.7 μg/mL	29.7%/10.5%
41	10 μM/24 μg/μL	10 μM/24 μg/mL	10 μM/24 μg/mL	1 μM/2.4μg/mL	not tested
42	30 μM/75 μg/μL	10 μM/25 μg/mL	3 μM/7.5 μg/mL	0.3 μM/ 0.75 μg/mL	not tested
43	3 μM/7.2 μg/μL	3 μM/7.2 μg/mL	10 μM/24 μg/mL	0.3 μM/0.72 μg/mL	not tested
44	30 μM/75 μg/μL	3 μM/7.8 μg/mL	10 μM/26 μg/mL	1 μm/2.6 μg/mL	not tested
45	3 μM/ 6.6 μg/μL	10 μm/22 μg/mL	100 μM/220 μg/μL	1 μM/2.2 μg/μL	not tested
46	3 μM/6.6 μg/mL	30 μM/66 μg/mL	100 μM/228 μg/mL	0.3 μM/0.66 μg/mL	not tested
47	10 μM/24 μg/mL	3 μM/7.2 μg/mL	10 μM/24 μg/mL	not tested	not tested
48	10 μM/24 μg/mL	10 μM/24 μg/mL	10 μM /24 μg/mL	not tested	not tested
49	30μM/75 μg/mL	10 μM/25 μg/mL	10 μM / 25 μg/mL	not tested	not tested
magainin-1 amide	30 μM	not active at 100 μM	not tested	not active at 100 μM	not tested
maginin-2 [52]		≥100 μg/mL		0.78 μM[54]	
NH_2-Lys4-magainin-2 [52]		≥100 μg/mL			
NH_2-Arg10-magainin-2[52]		25 μg/mL			
pexiganan[53]		16 μg/mL			
helical peptoid analogues of magainin-2 amide[55]					
analogue no. 1				> 100 μM	
analogue no. 2				7.8 μM	
analogue no. 5				0.82 μM	
analogue no. 7				>75 μM	

the in vivo mouse wound healing model, implying that these compounds stimulate the innate immune system. As seen in Table 3, compounds 23, 29, and 43 all caused significant increase in closure of wounds at all time points and exhibited a significant decrease in half closure time in the mouse cutaneous injury assay. In fact, these analogues exhibited activity very similar to that of the reference compound 2-*p*-[2-carboxyethyl]phenethylamino-5′-*N*-ethylcarboxamideadenosine, a potent adenosine A_2a receptor agonist that accelerates wound healing.[56,57]

In an attempt to determine if there is a correlation of hemolytic activity and toxicity, six of these compounds were evaluated in an in vivo mouse maximum tolerated dose study. The first four compounds (**27**−**30**) were evaluated at doses of 1, 5, and 25 mg/kg for 6 days, and none of these compounds exhibited any acute toxicity (Table 4). Two other compounds (**23** and **36**) were evaluated at 5, 25, and 125 mg/kg, and in both cases acute toxicity was observed at a dosage of 125 mg/kg. In the case of compound **23,** all animals lost weight and one animal died, while compound **36** exhibited much greater toxicity where 5 out of 5 animals died. It is interesting to note that for all six compounds at a dosing of 1, 5, and 25 mg/kg, no correlation between hemeolytic activity and acute toxicity was observed. Deslouches and co-workers[58] reported the synthesis of a series of peptides composed of repeating Arg and Val residues to induce an idealized amphipathic α-helix with selective substitution of Trp residues on the hydrophobic face of the helix to increase the overall hydrophobicity of the

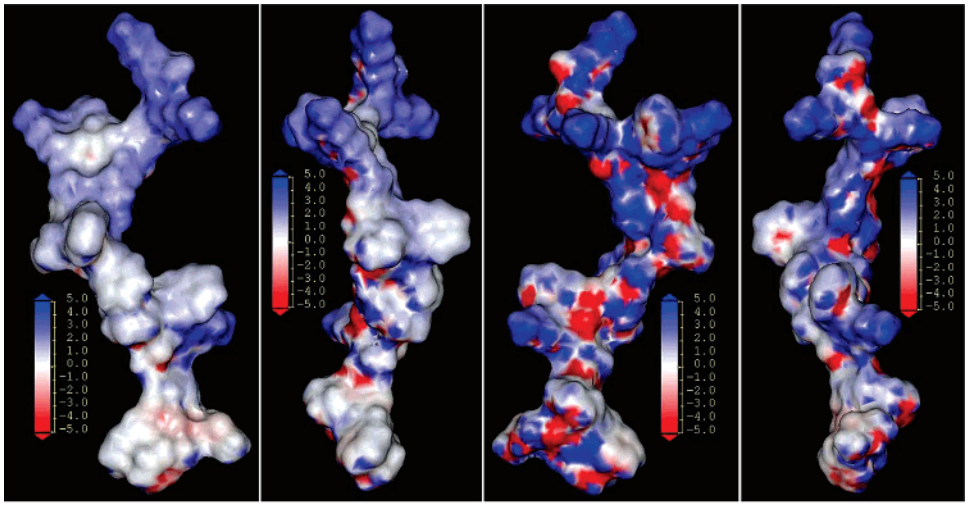

Figure 3. Electrostatic surface potential map of the active analogue **23** shows the polar and nonpolar faces of the molecule. Blue color indicates a positive charge. Red indicates a negative charge, and white indicates a neutral electric charge.

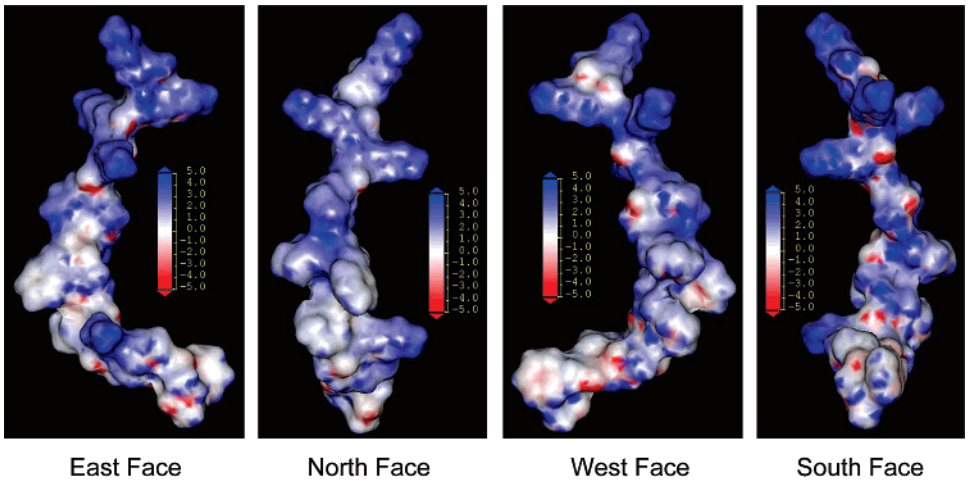

Figure 4. The electrostatic surface potential map of the much less active analogue **31** shows an even distribution of charge over the entire surface of the molecule. Blue color indicates a positive charge. Red indicates a negative charge, and white indicates a neutral electric charge.

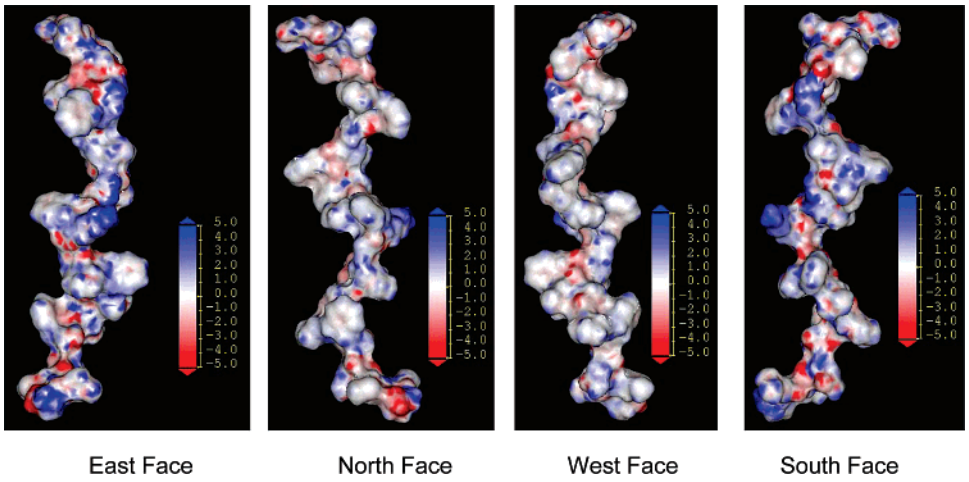

Figure 5. The effect of incorporation of the negatively charged pentapeptide (ELMNS) found at the C-terminus of the magainins at both the C and N terminus is shown by the electrostatic potential map of the completely inactive analogue **7**. Blue color indicates a positive charge. Red indicates a negative charge, and white indicates a neutral electric charge.

peptides. These very potent antibacterial compounds exhibited a maximum tolerated dose of only 16 mg/kg. The observed improvement in the maximum tolerated dose suggests that the incorporation of the Tic−Oic dipeptide does not allow these peptides to adopt an idealized amphipathic α-helical structure.

Table 3. Mouse Wound Healing Model Results

		wound healing, %					
compd	dose	day 3	day 5	day 7	day 9	day 11	CT_{50}
vehicle	20 μL/mouse	19.7	35.8	49.6	60.6	66.4	7.7 days
SEM[a]		4.9	3.4	3.0	0.9	0.9	0.2%
23	100 μg/mouse	36.3	51.5	63.3	69.8	77.5	6.1 days
SEM		1.9	2.9	1.6	2.0	2.3	0.2%
29	100 μg/mouse	39.7	54.1	64.9	72.7	79.0	5.7 days
SEM		2.3	3.0	2.0	0.6	0.6	0.2%
43	100 μg/mouse	38.8	51.2	67.2	72.8	81.1	5.7 days
SEM		3.1	2.1	1.1	1.6	1.5	0.1%
control[b]	10 μg/mouse	41.1	54.6	70.6	77.6	84.3	5.4 days
SEM		2.0	3.0	1.6	1.7	1.6	0.2%

[a] SEM is the deviation from the average % wound closure of the five animals within the specific group. [b] 2-*p*-[2-carboxyethyl]phenethylamino-5′-*N*-ethylcarboxamideadenosine is a potent adenosine A_2a receptor agonist that promotes wound healing and was used as the reference standard in this study.

Discussion

In order to systemically investigate the effects of varying the spacer and functional groups (Figure 1) on selectivity and potency for the three different bacterial strains, compound **23** was selected on the basis of its broad spectrum activity (activity against *Salmonella typhimurium* is 10 μM; activity against *Staphylococcus aureus* ME/GM/MTC resistant bacteria is 3 μM; activity against *Mycobacterium ranae* is 10 μM; activity against *Bacillus subtillis* is 1 μM coupled with relatively low hemolytic activity of 14%) as the reference compound for this investigation. The first hypothesis to be evaluated was the importance of the Tic−Oic dipeptide turn-inducing unit to antibacterial and hemolytic activity. In compound **31** the Tic residue was completely deleted from the sequence and resulted in loss of activity against *Staphylococcus aureus* ME/GM/MTC resistant bacteria and in a dramatic reduction in activity against *Salmonella typhimurium* from 10 to 100 μM and against *Mycobacterium ranae* from 10 to 100 μM. Hemolytic activity was also reduced to 6%. It is of interest to point out that compound **31** was still very active (3 μM) against the Gram-positive strain *Bacillus subtillis*. To determine whether the dramatic reduction in activity was due to the reduction of the overall amino acid sequence length from 19 to 15, compound **34** was prepared where all the Tic residues were replaced with Gly residues, thus maintaining the overall amino acid sequence length of 19. This resulted in the loss of activity against both *Salmonella typhimurium* and *Staphylococcus aureus* ME/GM/MTC resistant bacteria, while the activity against *Mycobacterium ranae* remained at 100 μM. Again, compound **34** was still relatively active (30 μM) against *Bacillus subtillis.* A reduction in hemolytic activity (3%) was also observed for this analogue. Two similar analogues were prepared by completely deleting the Oic residues in compound **32** or replacing it with a Gly residue to give compound **33**, resulting in loss of activity against *Staphylococcus aureus* ME/GM/MTC resistant bacteria and dramatic reduction in activity against *Salmonella typhimurium* (100 μM) while still maintaining relatively good activity against *Bacillus subtillis*. A reduction of hemolytic activity of (6%) was also observed. However, it is interesting to note that in both cases activity against *Mycobacterium ranae* was reduced only from 10 to 30 μM. This observation provides critical insight into the conformational and hydrophobic requirements for selective binding to the membranes of mycobacterium vs Gram-positive and Gram-negative bacterium. The final analogue prepared in the series was compound **35** where the Tic residue was replaced by the less conformationally restrained aromatic residue Phe, resulting in an analogue exhibiting antibacterial activity similar to that of compound **23**; however, a 2-fold increase in hemolytic activity (28%) was observed. This observation supports the hypothesis that in addition to playing the major role of inducing a turn conformation, the hydrophobicity of the Tic residue is also important for antibacterial activity and hemolytic activity.

Spacers 1 and 2 in compound **23** are both Gly residues; thus, there is only one carbon atom between the amide nitrogen atom and the carbonyl carbon atom of the amino acid residue. Compound **36** spacers 1 and 2 are both β-Ala residues containing a two-carbon spacer. This modification had little or no effect on the activity against all four bacterial strains; however, hemolytic activity increased to 25%. Compound **29** spacers 1 and 2 are both the amino acid GABA containing a three-carbon spacer. This modification had no effect on activity against *Salmonella typhimurium* or *Mycobacterium ranae*. However, the activity against *Staphylococcus aureus* ME/GM/MTC resistant bacteria was dramatically reduced from 3 to 100 μM. Hemolytic activity was approximately equal to compound **23**. Compound **37** spacers 1 and 2 are both 6-aminohexonic acid containing a five-carbon spacer. This modification had little or no effect on the activity against *Salmonella typhimurium* or *Staphylococcus aureus* ME/GM/MTC resistant bacteria or *Mycobacterium ranae*. However, the hemolytic activity increased to 45%. The final modification to spacers 1 and 2 was to delete this residue altogether in compound **28**. The deletion of both spacers 1 and 2 resulted in no change in the activity against *Salmonella typhimurium* and *Staphylococcus aureus* ME/GM/MTC resistant bacteria, with a very small increase in the

Table 4. Maximum Tolerated Dose Studies.

peptide	1 mg/kg	5 mg/kg	25 mg/kg	125 mg/kg	% hemolytic activity at 100 μM peptide
23	not tested	no observed toxicity	no observed toxicity	minor weight loss in 4 of 5 animals, 1 death	14
27	minor weight loss/ no observed toxicity	minor weight loss/ no observed toxicity	minor weight loss/ no observed toxicity	not tested	43
28	minor weight loss/ no observed toxicity	minor weight loss/ no observed toxicity	minor weight loss/ no observed toxicity	not tested	86
29	minor weight loss/ no observed toxicity	minor weight loss/ no observed toxicity	minor weight loss/ no observed toxicity	not tested	10
30	no observed toxicity	no observed toxicity	no observed toxicity	not tested	27
36	not tested	no observed toxicity	minor weight loss/ no observed toxicity	5 out of 5 animals died	25

activity against *Mycobacterium ranae*. The hemolytic activity, however, dramatically increased to 87%, making this compound the most toxic to red blood cells of the series tested. This data strongly suggest that spacers 1 and 2 play a major role in determining the conformational flexibility of these compounds. On the basis of the observation that compound **28** exhibits the highest hemolytic activity, coupled with the observation in the literature that helical character favors hemolytic activity,[3,15,16] one can postulate that the absence of spacers 1 and 2 reduces the conformational freedom of the peptide and induces a helical conformation onto the peptide, facilitating the binding to the membrane of red blood cells. The other spacers seem to exhibit, as one would expect, greater conformational freedom, allowing the peptide to adopt different conformations on interaction with red blood cells. In summary, spacers 1 and 2 seem to exhibit their greatest effect on hemolytic activity. As far as antibacterial activity is concerned, none of the spacers had a great effect except for GABA (**29**), which had a dramatic effect by reducing the activity by 33-fold against *Staphylococcus aureus* ME/GM/MTC resistant bacteria. This result implies that this spacer makes it more difficult for compound **29** to adapt, under the influence of the physicochemical properties of the *Staphylococcus aureus* cell membrane, a favorable binding conformation. This information may be critical in designing Gram-negative and mycobacterium selective agents.

Spacer 3 defines the distance from the side chain terminal amine group to the polypeptide backbone. To determine whether or not this distance has any affect on antibacterial activity, analogues with three different side chain lengths were investigated: compound **23** contains Lys residues with four methylene groups in the side chain; compound **43** contains Orn residues with three methylene groups in the side chain; compound **41** had only the C-terminal Lys residues replaced with Orn; compound **45** contains Dpr residues with two methylene groups in the side chain. The net result of this study was that these modifications had very little effect on activity against *Salmonella typhimurium* and *Staphylococcus aureus* ME/GM/MTC resistant bacteria; however, the activity against *Mycobacterium ranae* was dramatically reduced by 10-fold from 10 to 100 μM. This result indicates that inclusion of Dpr residues will increase selectivity for Gram-positive and Gram-negative bacteria vs mycobacterium with a 33-fold selectivity for Gram negative and a 10-fold selectivity for Gram positive bacteria vs mycobacteria.

It is known that the Phe residues participate in hydrophobic interactions with the hydrophobic core of the cell membrane. In an effort to determine whether changes in the electrostatic properties of Phe residue's aromatic ring do affect membrane binding, the 4-flurophenylalanine (Fpa) analogue **42** was prepared. The net result was a small decrease in activity against *Salmonella typhimurium* and *Staphylococcus aureus* ME/GM/MTC resistant bacteria with a small increase in the activity against *Mycobacterium ranae*. Replacement of the Phe residues with the much more electronegative 4-nitrophenylalanine (Nph) residues produced an analogue **49** with the same activity against *Salmonella typhimurium* and *Staphylococcus aureus* ME/GM/MTC resistant bacteria exhibited by **42**; however, this substitution resulted in a small decrease in the activity against *Mycobacterium ranae* (from 3 to 10 μM). This is a very interesting observation indicating that the hydrophobic interactions between these peptides and the membranes of mycobacterium are different in some way from the hydrophobic interactions with Gram-positive and Gram-negative membranes. Additional investigations are being carried out to fully understand this potential difference.

As seen in Table 2, various other modifications produced only small variations in the observed antibacterial activity. The *Bacillus subtillis* strain seems to be very insensitive to these subtle changes in structure and physicochemical properties. This assay may provide insight into the overall lethality of these compounds, but it provides very little insight into the physicochemical factors that define potency and selectivity. To date, compound **46**, containing β-Ala residues for spacers 1 and 2 and Dpr residues for spacer 3, exhibits the highest selectivity for *Salmonella typhimurium* with a 10-fold selectivity over *Staphylococcus aureus* ME/GM/MTC resistant bacteria and a 33-fold selectivity over *Mycobacterium ranae*. Compound **40** with a 3-fold selectivity over *Salmonella typhimurium* and a 10-fold selectivity over *Staphylococcus aureus* ME/GM/MTC resistant bacteria and compound **42** with a 10-fold selectivity over *Salmonella typhimurium* and a 3-fold selectivity over *Staphylococcus aureus* ME/GM/MTC resistant bacteria are the most selective analogues for *Mycobacterium ranae*. Compounds **2** and **4** are the only analogues to date that exhibit 10-fold or greater selectivity over *Staphylococcus aureus* ME/GM/MTC resistant bacteria versus *Salmonella typhimurium* and *Mycobacterium ranae*. However these compounds exhibit 100% hemolytic activity and are therefore not selective agents.

To rule out the possibility of the mechanism of action of these peptides involving a receptor mediated event, two analogues **47** and **48** incorporating D-Phe or D-Lys residues were prepared. It is well-established that a specific target or receptor for the membrane-disruptive AMPs is absent and is supported by the observation that analogues containing D-amino acid replacements do not exhibit reduced antibacterial activity.[59] As seen in Table 1, both analogues **47** and **48** exhibited the same activity against *Staphylococcus aureus* ME/GM/MTC resistant bacteria, *Salmonella typhimurium*, and *Mycobacterium ranae* as the reference compound **23** containing all L-amino acids. This observation is consistent with replacement studies, conducted by Bessalle and co-workers,[60] with the well characterized membrane disruptor magainin, which indicated no reduction in antibacterial activity even with 100% D-amino acid incorporation.

Conclusion

The results of this investigation clearly support the original hypothesis that AMPs interact differently with different bacterial strains such as Gram-positive, Gram-negative, and Mycobacterium bacteria because of the differing chemical composition of their respective cell membranes. Further, the results presented here show that small changes in the structural and physicochemical properties of the constituent amino acid residues can lead to major changes in the potency and selectivity of a particular AMP for a particular bacterial strain. Therefore, it should be possible, by careful selection and placement of residues with specific physicochemical properties, to design tailor-made AMPs with increased potency and selectivity for a specific strain of bacteria.

Experimental Section

NMR. All ^{1}H NMR data were collected using a Bruker Avance-600 spectrometer using a ^{1}H, ^{13}C, ^{15}N *z*-gradient cryoprobe. The samples of each peptide were prepared in (A) 100 mM SDS micelles and (B) 100 mM DPC micelles in 600 μL of 90% H_2O/10%D_2O buffered with 150 mM sodium acetate to a pH of 4.2. 1D ^{1}H NMR spectra were collected using the WATERGATE (water suppression by gradient tailored excitation) water suppression pulse sequence developed by Sklenar and co-workers.[61] Data were collected at a temperature of 300 K. A spectral width of 9090.9 Hz was used,

and data were acquired with 128k data points in F2. A total of 16 scans were collected for each spectrum. Spectra were processed using XWINNMR (Bruker) on a Hewlett-Packard workstation.

In Vitro Assays. All peptides were screened for antibacterial activity in the following four in vitro assays: (1) *Salmonella, typhimurium* (ATCC 13311) Gram-negative,[62,63] (2) *Staphylococcus aureus* methicillin/gentamicin/tetracycline resistant (ATCC 33592) Gram-positive,[64] (3) *Bacillus subtillis* (ATCC 43223) Gram-positive,[62,63] and (4) *Mycobacterium ranae* (ATCC 110)[62,63] by MDS Pharma Services using the following protocol. The test substance/vehicle was added to test wells containing the selected microorganisms (1×10^{-4} to 5×10^{-5} CFU/mL) in the appropriate culture medium under controlled conditions. Final incubation concentration was determined by comparison to a reference standard optical density curve. After 1−4 days, growth of the culture was examined and scored positive (+) for inhibition of growth or turbidity and negative (−) for no effect upon growth or turbidity. Samples were evaluated at concentrations of 100, 30, 10, 3, 1, 0.3, and 0.1 μM in 1% DMSO to determine the minimal inhibitory concentration.

In Vivo Assays. Selected compounds were evaluated in an in vivo mouse skin wound healing model by MDS Pharma Services using the following protocol. Groups of CD-1 derived male mice ($n = 5$) weighing 24 ± 2 g were used. Under hexabarbitol (90 mg/kg, ip) anesthesia, the shoulder and back region of each animal was shaved. A sharp punch (i.d. of 12 mm) was applied to remove the skin including *panniculus carnosus* and adherent tissues. Test substances at a concentration of 100 μg/mouse were each administered topically immediately following cutaneous injury, once daily for 10 consecutive days. The wound area, traced onto clear plastic sheets, was measured by use of an Image-ProPlus (Media Cybernetics, version 4.5.0.29) on days 1, 3, 5, 7, 9, and 11. The percent closure of the wound was calculated, and wound half-closure time (CT_{50}) was analyzed by linear regression using GraphPad Prism (GraphPad Software, San Diego, CA). One-way ANOVA followed by Dunnett's test was applied for comparison between the treated and its corresponding vehicle groups at each measurement time point. Differences were considered statistically significant at $P < 0.05$.[65]

Maximum Tolerated Dose. Six compounds were evaluated in an in vivo mouse model to determine the maximum tolerated dose for each compound by BIOCON, Inc., using the following protocol. For each compound, three dose concentrations (1, 5, and 25 mg/kg or 1, 5, and 125 mg/kg) were administered ip 1−2 times per day as split doses: day "0", weigh the animals; days 1−6, dose daily and observe animals; day 7, weigh, euthanize, and necrotize to examine abdominal cavity.

Hemolytic Studies. An amount of 5 mL of blood was taken and spun down at 2500 rpm for 5 min. The supernatant was decanted, washed with PBS (20 mL each time, pH 7.4, isotonic) six times or until the supernatant became clear, and resuspended in 125 mL of PBS to obtain a 4% count. An amount of 500 μL each was used for the experiments.

Peptide Synthesis. All of the above-mentioned peptides were synthesized at 60 μM scale using an Advanced Chemtech ACT 396 model multiple peptide synthesizer. Standard Fmoc chemistry was followed for the synthesis.[66−68] Rink amide MBHA resins [4(2′,4′-dimethoxyphenyl-Fmoc-aminomethyl)phenoxyacetamido-L-norleucyl-*p*-methylbenzhydrylamine resin] (purchased from NovaBioChem) were used as the solid phase and DMF (dimethyl formamide) was used as the primary transfer and wash solvent. A 20% piperidine solution in DMF was used for deprotection. A solution of HBTU (*O*-benzotriazole-*N*,*N*,*N*′,*N*′-tetramethyluroniumphosphate) in conjunction with HOBT (1-hydroxybenzotriazole) in DMF was used as the coupling agent, and 5% acetic anhydride in DMF was used for capping. DIPEA (diisopropylethylamine, 2 M in *N*-methylmorpholine) was used as the tertiary amine in the coupling step. All amino acids were dissolved in NMM (*N*-methylmorpholine). Upon completion of the synthesis, the resin was thoroughly washed with methanol (5 times), dried overnight under high vacuum (0.05 Torr), and cleaved using a cocktail containing TFA (88%), water (5%), phenol (5%), and triisopropylsilane (2%) for 3 h. This mixture of resin and cleave cocktail was filtered followed by addition to cold (−20 °C) stabilizer-free dry diethyl ether. The precipitated peptide was centrifuged, and the supernatant was removed. This pellet of peptide was repeatedly washed with dry diethyl ether (20 mL × 2) and dried overnight under high vacuum (0.05 Torr). The crude peptide thus obtained was dissolved in 0.1% TFA (trifluoroacetic acid), and a 1% aliquot was saved for HPLC, mass spectrometry, and other analyses. These crude peptides were purified by reverse-phase HPLC for further applications.

Peptide Purification and Analyses. All HPLC analyses were carried out using an Agilent 1100 series analytical instrument (equipped with autosampler and diode array detector) and a Vydac C18 narrow bore reverse-phase column (250 mm × 2.1 mm, 5 μM particle size, 100 μL/min flow rate). The mobile phase A consisted of water (97.5%, containing 0.5 mL TFA) and 2-propanol (2.5%), while mobile phase B consisted of MeCN (88.88%), water (8.88%, containing 0.4 mL of TFA), and 2-propanol (2.4%). All analyses were carried out under gradient conditions (1−90% B over 60 min) at a flow rate of 100 μL/min. All crude peptides were purified to 97% or more for analytical and other experimental purposes. All preparative purifications were carried out using an Agilent 1100 series preparative instrument and a Vydac C18 reverse-phase preparative column (250 mm × 22 mm, 10 μM particle size, 10 mL/min flow rate) using the same mobile phases. All purified peptides were analyzed again by HPLC and mass spectrometry. Mass Spectral analyses were carried out using a Finnigan LTQ ESI-MS instrument running Xcalibur 1.4SR-1 or a Kratos PC Axima CFR Plus instrument (MALDI) running Kompact V2.4.1. ESI-MS showed multiply charged ions, and the accurate mass was calculated. MALDI analyses were performed in reflectron mode, and hence, in most cases the $(M + H)^+$ ion corresponding to the monoisotopic mass was observed (Supporting Information, Table 1). In the case of compounds showing only $(M + Na)^+$ or $(M + K)^+$ peaks, the mass was confirmed by running the same experiment in negative ion mode.

Molecular Modeling. Cerius2 (C2), version 4.9,[69] and InsightII, version 2001,[70] running on a Silicon Graphics Octane workstation under the IRIX 6.5 operating system were used for all of the modeling calculations presented here. Gasteiger[71] charges with consistent force field[72] was used for all of the computations employing involving C2, and consistent valence force field (CVFF) was used for all computations employing InsightII. Unless otherwise noted, default C2 and InsightII parameters were used. Each peptide was built using the Biopolymer module; the resulting structure was minimized using steepest descent algorithm[73] after a brief molecular dynamics simulation run. These structures were then subjected to a conformational search algorithm using the Boltzmann jump method[74] as implemented in C2 to obtain a series of minimum energy conformers. The parameters used in this search were as follows: Torsion window was fixed to 120, temperature was set to 5000 K, and the number of perturbations was set to 50. The torsion bond is defined as a single bond connecting different groups, which on rotation would give rise to a potential local minimum conformer. Cluster analysis was performed on the basis of the rms (root mean square) differences of the torsion angles between the conformers. Electrostatic potential surfaces for selected AMP conformers were computed as follows. The electrostatic potential for each conformer was computed employing a grid with origin at its grid points, resolution of 65 points per axis, and solute extending to 80 Å. The solute was defined with Gasteiger charges, van der Waals radii, dielectric constant of 2.0, and point charge distribution. The solvent dielectric constant was set to 80, solvent radii were set to 1.4 Å, ionic strength was set to 0.145, and the ionic radii were set to 2.0 Å. The molecular surfaces computed were Connolly surfaces with solid display style, using atom radii scale of 1.0, atom radii increment of 0.0, and probe radius of 1.4 Å. The surfaces were colored with Delphi spectrum using the electrostatic potential grid as the coloring method.

Acknowledgment. The authors acknowledge funding from the Bacterial Therapeutics Program 2.1 of the Defense Threat Reduction Agency. Material in this document is covered by U.S. Provisional Patent Application serial number 60/876,377 assigned to the United States Army. The authors thank Drs. Fong-Chi Cheng, Ching-Chui Lin, and Keng-Kuang Chang of MDS Pharma Services for conducting the in vitro antibacterial studies and in vivo mouse healing studies; and Dr. Frank Klotz of Biocon Inc. for conducting the in vivo maximum tolerated dose studies. This research was performed while one of the authors (J.B.B.) held a National Research Council Research Associateship Award at Walter Reed Army Institute of Research. Material has been reviewed by the Walter Reed Army Institute of Research. There is no objection to its presentation and/or publications. The opinions or assertions contained herein are the private views of the authors, and are not to be construed as official, or as reflecting true views of the Department of the Army or the Department of Defense.

Supporting Information Available: Mass spectral data for the compounds synthesized in our laboratory. This material is available free of charge via the Internet at http://pubs.acs.org.

References

(1) Yeaman, M. R.; Yount, N. Y. Mechanisms of antimicrobial peptide action and resistance. *Pharmacol. Rev.* **2003**, *55* (1), 27−55.
(2) Dennison, S. R.; Wallace, J.; Harris, F.; Phoenix, D. A. Amphiphilic α-helical antimicrobial peptides and their structure/function relationships. *Protein Pept. Lett.* **2005**, *12*, 31−39.
(3) Toke, O. Antimicrobial peptides; new candidates in the fight against bacterial infections. *Biopolymers* **2005**, *80*, 717−735.
(4) Ganz, T. Defensins: antimicrobial peptides of innate immunity. *Nat. Rev. Immunol.* **2003**, *3*, 710−720.
(5) Simmaco, M.; Mignogna, G.; Barra, D. Antimicrobial peptides from amphibian skin: what do they tell us? *Biopolymers* **1999**, *47*, 435−450.
(6) Hancock, R. E. W.; Lehrer, R. Cationic peptides: a new source of antibiotics. *Trends Biotechnol.* **1998**, *16*, 82−88.
(7) Zasloff, M. Antimicrobial peptides of multi-cellular organisms. *Nature* **2002**, *415*, 389−395.
(8) Powers, J.-P. S.; Hancock, R. E. W. The relationship between peptide structure and antibacterial activity. *Peptides* **2003**, *24*, 1681−1691.
(9) Brogden, K. A. Antimicrobial peptides: pore formers or metabolic inhibitors in bacteria? *Nat. Rev. Microbiol.* **2005**, *3*, 238−250.
(10) Tossi, A.; Sandri, L.; Giangaspero, A. Amphipathic α-helical antimicrobial peptides. *Biopolymers* **2000**, *55*, 4−30.
(11) Hicks, R. P.; Mones, E.; Kim, H.; Koser, B. W.; Nichols, D. A.; Bhattacharjee, A. K. Comparison of the conformation and electrostatic surface properties of magainin peptides bound to SDS and DPC micelles: Insight into possible modes on antimicrobial activity. *Biopolymers* **2003**, *68*, 459−470.
(12) Song, Y. M.; Park, Y.; Lim, S. S.; Yang, S.-T.; Woo, E.-R.; Park, S.; Lee, J. S.; Kim, J. I.; Hahm, K.-S.; Kim, Y.; Shin, S. Y. Cell selectivity and mechanism of action of antimicrobial model peptides containing peptoid residues. *Biochemistry* **2005**, *44*, 12094−12106.
(13) Papo, N.; Shai, Y. Effects of drastic sequence alteration and D-amino acid incorporation on the membrane binding behavior of lytic peptides. *Biochemistry* **2004**, *43*, 6393−6403.
(14) Dathe, M.; Meyer, J.; Beyerman, M.; Maul, B.; Hoischen, C.; Bienert, M. General aspects of peptide selectivity towards lipid bilayers and cell membrane studied by variation of structural parameters of amphipathic α-helical model peptides. *Biochim. Biophys. Acta* **2002**, *1558*, 171−186.
(15) Chen, Y.; Mant, C. T.; Farmer, S. W.; Hancock, R. E.; Vasil, M. L.; Hodges, R. S. Rational design of α-helical antimicrobial peptides with enhanced activities and specificity/therapeutic index. *J. Biol. Chem.* **2005**, *280*, 12316−12329.
(16) Oren, Z.; Hong, J.; Shai, Y. *J. Biol. Chem.* **1997**, *272*, 14643−14649.
(17) Dathe, M.; Wiencek, J. M. Structural features of helical antimicrobial peptides: their potential to modulate activity on model membranes and biological cells. *Biochim. Biophys. Acta* **1999**, *1462*, 71−87.
(18) Blondelle, S. E.; Lohneer, K.; Aguilar, M. Lipid-induced conformation and lipid-binding properties of cytolytic and antimicrobial peptides: determination and biological specificity. *Biochim. Biophys. Acta* **1999**, *1462*, 89−108.
(19) Papo, N.; Shai, Y. Can we predict biological activity of antimicrobial peptides from their interaction with model phospholipid membranes? *Peptides* **2003**, *24*, 1693−1703.
(20) Pouny, Y.; Rapaport, D.; Mor, A.; Nicolas, P.; Shai, Y. Interaction of antimicrobial dermaseptin and fluorescently labeled analogues with phospholipid membranes. *Biochemistry* **1992**, *31*, 12416−12423.
(21) Bechinger, B. Solid-state NMR investigations of the interaction contributions that determine the alignment of helical polypeptides in biological membranes. *FEBS Lett.* **2001**, *504*, 161−165.
(22) Lee, M. T.; Chen, F. Y.; Haung, H. W. Energetics of pore formation induced by membrane active peptides. *Biochemistry* **2004**, *43*, 3590−3599.
(23) Papo, N.; Shai, Y. New lytic peptides based on the D,L amphipathic helix motif preferentially kill tumor cells compared to normal cells. *Biochemistry* **2003**, *42*, 9346−9354.
(24) Yeaman, N. R.; Yount, N. Y. Mechanisms of antimicrobial peptide action and resistance. *Pharmacol Rev.* **2003**, *55* (1), 27−55.
(25) Giangaspero, A.; Sandri, L.; Tossi, A. Amphipathic α-helical antimicrobial peptides. *Eur. J. Biochem.* **2001**, *268*, 5589−5600.
(26) Azuma, I.; Yamamura, Y.; Tanaka, Y.; Kohsaka, K.; Mori, T.; Itoh, T. Cell wall of *Mycobacterium lepraemurium* strain Hawaii. *J. Bacteriol.* **1973**, *113* (1), 515−518.
(27) Glukhov, E.; Stark, M.; Burrows, L. L.; Deber, C. M. Basis for selectivity of cationic antimicrobial peptides for bacterial versus mammalian membranes. *J. Biol. Chem.* **2005**, *280*, 33960−33967.
(28) Zasloff, M. Antimicrobial peptides of multicellular organisms. *Nature* **2002**, *415*, 389−395.
(29) Matsuzaki, K. Magainins as paradigm for the mode of action of pore forming polypeptides. *Biochim. Biophys. Acta* **1998**, *1376*, 391−400.
(30) Wenk, M. R.; Seelig, J. Magainin 2 amide interaction with lipid membranes: calorimetric detection of peptide binding and pore formation. *Biochemistry* **1998**, *37*, 3909−3916.
(31) Yang, L.; Weiss, T. M.; Lehrer, R. I.; Huang, H. W. Crystallization of antimicrobial pores in membranes: magainin and protegrin. *Biochem. J.* **2000**, *79*, 2002−2009.
(32) Anderson, A.; Maler, L. Motilin−bicelle interactions: membrane position and translation and diffusion. *FEBS Lett.* **2003**, *545*, 139−143.
(33) Corzo, G.; Escoubas, P.; Villegas, E.; Barnham, K. J.; He, W.; Norton, R. S. Characterization of unique amphipathic antimicrobial peptides from venom of the scorpion pandinus imperator. *Biochem. J.* **2001**, *359*, 35−45.
(34) Epand, R. F.; Umezawa, N.; Porter, E. A.; Gellman, S. H.; Epand, R. M. Interactions of the antimicrobial β-peptide B-17 with phospholipid vesicles differ from membrane interactions of magainins. *Eur. J. Biochem.* **2003**, *270*, 1240−1248.
(35) Mulkerrin, M. G. Protein Structure Analysis Using Circular Dichroism. In *Spectroscopic Methods for Determining Protein Structure in Solution*; Havel, H. A., Ed.; VCH: New York, 1996.
(36) Surewicz, W. K.; Mantsch, H. H. Infrared Absorption Methods for Examining Protein Structure. In *Spectroscopic Methods for Determining Protein Structure in Solution*; Havel, H. A., Ed.; VCH: New York, 1996; pp 135−162.
(37) Tensmeyer, L. G.; Kauffman, E. W. Protein Structure As Revealed by Nonresonance Raman Spectroscopy. In *Spectroscopic Methods for Determining Protein Structure in Solution*; Havel, H. A., Ed.; VCH: New York, 1996; pp 96−134.
(38) Whitehead, T. L.; McNair, S. D.; Hadden, C. E.; Young, J. K.; Hicks, R. P. Membrane-induced secondary structures of neuropeptides: a comparison of the solution conformations adopted by agonists and antagonists of the mammalian tachykinin NK1 receptor. *J. Med. Chem.* **1998**, *41* (9), 1497−506.
(39) Whitehead, T. L.; Hicks, R. P. Rationale for using simple and complex micelles in polypeptide conformational analysis. *Recent Res. Dev. Med. Chem.* **2001**, *1*, 213−233.
(40) Perrine, S. A.; Whitehead, T. L.; Hicks, R. P.; Szarek, J. L.; Krause, J. E.; Simmons, M. A. Solution structures in SDS micelles and functional activity at the bullfrog substance P receptor of ranatachykinin peptides. *J. Med. Chem.* **2000**, *43* (9), 1741−53.
(41) Young, J. K.; Hicks, R. P. NMR and molecular modeling investigations of the neuropeptide bradykinin in three different solvent systems: DMSO, 9:1 dioxane/water, and in the presence of 7.4 mM lyso phosphatidylcholine micelles. *Biopolymers* **1994**, *34* (5), 611−23.
(42) Jing, W.; Hunter, H. N.; Hagel, J.; Vogel, H. J. The structure of the antimicrobial peptide Ac-RRWWRF-NH_2 bound to micelles and its interactions with phospholipid bilayers. *J. Pept. Res.* **2003**, *61*, 219−229.

(43) Watson, R. M.; Woody, R. W.; Lewis, R. V.; Bohle, D. S.; Andreotti, A. H.; Ray, B.; Miller, K. W. Conformational changes in pediocin AcH upon vesicle binding and approximation of the membrane-bound structure in detergent micelles. *Biochemistry* **2001**, *40*, 14037−14046.
(44) Whitehead, T. L.; Jones, L. M.; Hicks, R. P. Effects of the incorporation of CHAPS into SDS micelles on neuropeptide−micelle binding: separation of the role of electrostatic interactions from hydrophobic interactions. *Biopolymers* **2001**, *58* (7), 593−605.
(45) Whitehead, T. L.; Jones, L. M.; Hicks, R. P. PFG-NMR investigations of the binding of cationic neuropeptides to anionic and zwitterionic micelles. *J. Biomol. Struct. Dyn.* **2004**, *21* (4), 567−576.
(46) Kyle, D. J.; Blake, P. R.; Smithwick, D.; Green, L. M.; Martin, J. A.; Sinsko, J. A.; Summers, M. F. NMR and computational evidence that high-affinity bradykinin receptor antagonists adopt C-terminal beta-turns. *J. Med. Chem.* **1993**, *36* (10), 1450−1460.
(47) Giacometti, A.; Cirioni, O.; Del Prete, M. S.; Paggi, A. M.; D'Errico, M. M.; Scalise, G. Combination studies between polycationic peptides and clinically used antibiotics against Gram-positive and Gram-negative bacteria. *Peptides* **2000**, *21*, 1155−1160.
(48) Grgurina, I.; Bensaci, M.; Pocsfalvi, G.; Mannina, L.; Cruciani, O.; Fiore, A.; Fogliano, V.; Sorensen, K. N.; Takemoto, J. Y. Novel cyclic lipodepsipeptide from *Pseudomonas syringae* pv. lachrymans strain 508 and Syringopeptin antimicrobial activities. *Antimicrob. Agents Chemother.* **2005**, *49* (12), 5037−5045.
(49) Lockwood, N. A.; Haseman, J. R.; Tirrell, M. V.; Mayo, K. H. Acylation of SC4 dodecapeptide increases bactericidal potency against Gram-positive bacteria, including drug-resistant strains. *Biochem. J.* **2004**, *378*, 93−103.
(50) Giacometti, A.; Cirioni, O.; Del Prete, M. S.; Barchiesi, F.; Paggi, A. M.; Petrelli, E.; Scalise, G. Comparative activities of polycationic peptides and clinically used antimicrobial agents against multi-drug-resistant nosocomial isolates of Acinetobacter baumannii. *J. Antimicrob. Chemother.* **2000**, *46*, 807−810.
(51) Patch, J. A.; Barron, A. E. Helical peptoid mimics of magainin-2 amide. *J. Am. Chem. Soc.* **2003**, *125*, 12092−12093.
(52) Bessalle, R.; Haas, H.; Goria, A.; Shalit, I.; Fridkin, M. Augmentation of the antibacterial activity of magainin by positive-charge chain extension. *Antimicrob. Agents Chemother.* **1992**, *36* (2), 313−317.
(53) Ge, Y.; MacDonald, D. L.; Holroyd, K. J.; Thornsberry, C.; Wexler, H.; Zasloff, M. In vitro antibacterial properties of pexiganan an analog of magainin. *Antimicrob. Agents Chemother* **1999**, *43* (4), 782−788.
(54) Kim, H. K.; Lee, D. G.; Park, Y.; Kim, H. N.; Choi, B. H.; Choi, C.-H.; Hahn, K.-S. Antibacterial activities of peptides designed as hybrids of antimicrobial peptides. *Biotechnol. Lett.* **2002**, *24*, 347−353.
(55) Patch, J. A.; Barron, A. E. Helical peptoid mimics of magainin-2 amide. *J. Am. Chem. Soc.* **2003**, *125*, 12092−12093.
(56) Montesinos, M. C.; Gadangi, P.; Longaker, M.; Sung, J.; Levine, J.; Nilsen, D.; Reibman, J.; Li, M.; Jiang, C. K.; Hirschhorn, R.; Recht, P. A.; Ostad, E.; Levin, R. I.; Cronstein, B. N. Wound healing is accelerated by agonists of adenosine A2 (G alpha s-linked) receptors. *J. Exp. Med.* **1997**, *186* (3), 1615−1620.
(57) Desai, A.; Victor-Vega, C.; Gadangi, S.; Montesinos, M. C.; Chu, C. C.; Cronstein, B. N. Adenosine a2a receptor stimulation increases angiogenesis by down-regulating production of the antiangiogenic matrix protein thrombospondin 1. *Mol. Pharmacol.* **2005**, *67* (5), 1406−1413.
(58) Deslouches, B.; Islam, K.; Craigo, J. K.; Montelaro, S. M. P.; Mietzner, T. A. Activity of the de novo engineered antimicrobial peptide WLBU2 against pseudomonas aeruginosa in human serum and whole blood for systemic applications. *Antimicrob. Agents Chemother.* **2005**, *49* (8), 3208−3216.
(59) Matsuzaki, K. Why and how are peptide−lipid interactions utilized for self-defense? Magainins and tachyplesins as archetypes. *Biochim. Biophys. Acta* **1999**, *1462*, 1−10.
(60) Bessalle, R.; Kapitkovsky, A.; Gorea, A.; Shalit, I.; Fridkin, M. All D-magainin: chirality, antimicrobial activity and proteolytic resistance. *FEBS Lett.* **1990**, *274*, 151−155.
(61) Sklenar, M.; Piotto, M.; Leppik, R.; Saudek, V. Gradient-tailored water suppression for $^{1}H-^{15}N$ HSQS experiments optimized to retain full sensitivity. *J. Magn. Res., Ser. A* **1993**, *102*, 241.
(62) Di, Modugno, E.; Erbetti, I.; Ferrari, L.; Galassi, G.; Hammond, S. M.; Xerri, L. In vitro activity of the tribactam GV 104326 against Gram-positive, Gram-negative and anaerobic bacteria. *Antimicrob. Agents Chemother.* **1994**, *38*, 2362−2368.
(63) Misiek, M.; Pursiano, T. A.; Leitner, F.; Price, K. E. Microbiological properties of a new cephalosporin, BL-S 339: 7-(phenylacetyimidoyl-aminoacetamido)-3-(2-methyl-1,3,4-thiadiazol-5-ylthiomethyl)ceph-3-em-4-carboxylic acid. *Antimicrob. Agents Chemother.* **1973**, *3*, 40−48.
(64) Edwards, J. R.; Turner, P. J.; Withnell, E. S.; Grindy, A. J.; Narin, K. In vitro antibacterial activity of SM-7338, a carbapenem antibiotic with stability to dehydropeptidase 1. *Antimicrob. Agents Chemother.* **1989**, *33* (2), 215−222.
(65) Montesinos, M. C.; Gadangi, P.; Longaker, M.; Sung, J.; Levine, J.; Nilsen, D.; Reibman, J.; Li, M.; Jiang, C.-K.; Hirschhorn, R.; Recht, P. A.; Ostad, E.; Levin, R. I.; Cronstein, B. N. Wound healing is accelerated by agonists of adenosine A_2 (G_{xs}-linked) receptors. *J. Exp. Med.* **1997**, *186*, 1615−1620.
(66) Grant, G. A. *Synthetic Peptides. A User's Guide*, 2nd ed.; Oxford University Press: New York, 2002.
(67) Benoiton, N. L. *Chemistry of Peptide Synthesis*; Taylor and Francis (CRC Press): Boca-Raton, FL, 2006.
(68) Schmidt, J. J.; Stafford, R. G.; Millard, C. B. High-throughput assays for botulinum neurotoxin proteolytic activity: serotypes A, B, D, and F. *Anal. Biochem.* **2001**, *296* (1), 130−137.
(69) *Cerius2 Modeling Environment*, release 4.9; Accelrys Software, Inc.: San Diego, CA, 2005.
(70) *InsightII Molecular Modeling Software*, version 2000.1; Accelrys Software, Inc.: San Diego, CA, 2005.
(71) Marsili, M.; Gasteiger, J. Fast calculation of atomic charges from molecular topology and orbital electronegativies. *Stud. Phys. Theor. Chem.* **1981**, *16*, 56−67.
(72) Mayo, S. L.; Olafson, B. D.; Goddard, W. A. I. DREIDING: a generic force field. *J. Phys. Chem.* **1990**, *94*, 8897−8909.
(73) Levitt, M.; Lifson, S. Refinement of protein conformations using a macromolecular energy minimization procedure. *J. Mol. Biol.* **1969**, *46* (2), 269−279.
(74) Chang, G.; Guida, W. C.; Still, W. C. An internal-coordinate Monte Carlo method for searching conformational space. *J. Am. Chem. Soc.* **1989**, *111*, 4379−4386.

JM061489V